



Overview of the RGD-Based PET Agents Use in Patients With Cardiovascular Diseases: A Systematic Review

Matthieu Dietz^{1,2}, Christel H. Kamani^{1,3}, Vincent Dunet^{4,5}, Stephane Fournier^{3,5}, Vladimir Rubimbura³, Nathalie Testart Dardel¹, Ana Schaefer¹, Mario Jreige⁴, Sarah Boughdad¹, Marie Nicod Lalonde^{1,5}, Niklaus Schaefer^{1,5}, Nathan Mewton^{2,6,7}, John O. Prior^{1,5*} and Giorgio Treglia^{1,5,8,9}

¹ Nuclear Medicine and Molecular Imaging Department, Lausanne University Hospital, Lausanne, Switzerland, ² INSERM U1060, CarMeN Laboratory, University of Lyon, Lyon, France, ³ Cardiology Department, Lausanne University Hospital, Lausanne, Switzerland, ⁴ Department of Diagnostic and Interventional Radiology, Lausanne University Hospital, Lausanne, Switzerland, ⁵ University of Lausanne, Lausanne, Switzerland, ⁶ Cardiovascular Hospital Louis Pradel, Department of Heart Failure, Hospices Civils de Lyon, Lyon, France, ⁷ Clinical Investigation Center Inserm 1407, Lyon, France, ⁸ Clinic of Nuclear Medicine, Imaging Institute of Southern Switzerland, Ente Ospedaliero Cantonale, Bellinzona, Switzerland, ⁹ Università della Svizzera Italiana, Lugano, Switzerland

OPEN ACCESS

Edited by:

Domenico Albano,
University of Brescia, Italy

Reviewed by:

Matteo Bauckneht,
Università di Genova, Italy
Francesco Fìz,
Ente Ospedaliero Ospedali
Galliera, Italy
Florent L. Besson,
Université Paris-Saclay, France

*Correspondence:

John O. Prior
john.prior@chuv.ch

Specialty section:

This article was submitted to
Nuclear Medicine,
a section of the journal
Frontiers in Medicine

Received: 02 March 2022

Accepted: 19 April 2022

Published: 06 May 2022

Citation:

Dietz M, Kamani CH, Dunet V, Fournier S, Rubimbura V, Testart Dardel N, Schaefer A, Jreige M, Boughdad S, Nicod Lalonde M, Schaefer N, Mewton N, Prior JO and Treglia G (2022) Overview of the RGD-Based PET Agents Use in Patients With Cardiovascular Diseases: A Systematic Review. *Front. Med.* 9:887508. doi: 10.3389/fmed.2022.887508

Studies using arginine–glycine–aspartate (RGD)-PET agents in cardiovascular diseases have been recently published. The aim of this systematic review was to perform an updated, evidence-based summary about the role of RGD-based PET agents in patients with cardiovascular diseases to better address future research in this setting. Original articles within the field of interest reporting the role of RGD-based PET agents in patients with cardiovascular diseases were eligible for inclusion in this systematic review. A systematic literature search of PubMed/MEDLINE and Cochrane library databases was performed until October 26, 2021. Literature shows an increasing role of RGD-based PET agents in patients with cardiovascular diseases. Overall, two main topics emerged: the infarcted myocardium and atherosclerosis. The existing studies support that $\alpha_v\beta_3$ integrin expression in the infarcted myocardium is well evident in RGD PET/CT scans. RGD-based PET radiotracers accumulate at the site of infarction as early as 3 days and seem to be peaking at 1–3 weeks post myocardial infarction before decreasing, but only 1 study assessed serial changes of myocardial RGD-based PET uptake after ischemic events. RGD-based PET uptake in large vessels showed correlation with CT plaque burden, and increased signal was found in patients with prior cardiovascular events. In human atherosclerotic carotid plaques, increased PET signal was observed in stenotic compared with non-stenotic areas based on MR or CT angiography data. Histopathological analysis found a co-localization between tracer accumulation and areas of $\alpha_v\beta_3$ expression. Promising applications using RGD-based PET agents are emerging, such as prediction of remodeling processes in the infarcted myocardium or detection of active atherosclerosis, with potentially significant clinical impact.

Keywords: $\alpha_v\beta_3$ integrin, RGD, angiogenesis, positron emission tomography, cardiovascular diseases, myocardial infarction, atherosclerosis

INTRODUCTION

Ischemic heart disease is the leading cause of death worldwide (1). Understanding cellular alterations involved in atherosclerotic plaque instability, as well as reparative mechanisms following myocardial infarction (MI) is important for both preventive and therapeutic intervention.

Positron emission tomography (PET) is an *in vivo* medical imaging technique that enables quantification of radiotracer uptake in the entire body at a cellular level.

Integrin $\alpha_v\beta_3$ is a transmembrane receptor mediating cell adhesion that influences cell growth, proliferation, survival, and migration. The peptide motif arginine-glycine-aspartate, abbreviated by “RGD” in the one-letter code, has been identified in 1984 as a minimal amino acid sequence that some integrins recognize in their natural ligands (2). In 1991 a group from Germany reported a strong and selective binding of cyclic pentapeptides containing the RGD sequence to $\alpha_v\beta_3$ integrin (3). The past 20 years have witnessed a remarkable expansion on cyclic peptides containing the RGD sequence since it was found that $\alpha_v\beta_3$ integrin plays a major role in angiogenesis, further enhanced by the first successful clinical applications of the PET radiopharmaceutical ^{18}F -Galacto-RGD (4–8).

The integrin-mediated cell adhesion/migration imaging with RGD PET was found to be involved in a wide range of pathophysiological processes, not only related to angiogenesis. Increased $\alpha_v\beta_3$ expression has been observed in some cancer cells as well as in cells involved in extracellular matrix remodeling such as fibroblasts and activated macrophages (8, 9). However, the clinical relevance of such biomarker is not well understood (8). Although most studies using RGD-PET agents focused predominantly on tumorigenesis, a greater focus on non-oncological applications such as cardiovascular diseases is of interest (9). In fact, in the development of atherosclerosis, expression of integrin $\alpha_v\beta_3$ has been found in endothelial cells as well as in CD68-positive macrophages, which are known as key factors in plaque instability (10–12). Moreover, $\alpha_v\beta_3$ integrin expression seems to appear central to the coordination of myocardial repair following MI. $\alpha_v\beta_3$ integrin is indeed upregulated in states of angiogenesis within the infarcted myocardium and could be expressed by activated myofibroblasts and macrophages during margination and chemotaxis (13, 14).

Some recent studies using RGD-PET agents in cardiovascular diseases have been published. The aim of this systematic review is to perform an updated evidence-based summary about the role of RGD-based PET agents in patients with cardiovascular diseases to better address further research in this setting.

MATERIALS AND METHODS

The reporting of this systematic review conforms to the updated “Preferred Reporting Items for a Systematic Review and Meta-Analysis” (PRISMA) statement, an established guidance to identify, select, appraise, and synthesize studies in systematic reviews (15).

Search Strategy

A comprehensive computer literature search of PubMed/MEDLINE, and Cochrane library databases was performed by two authors (MD and GT) to identify published articles that investigated the role of RGD-based PET agents in patients with cardiovascular diseases. A combination of the following terms was used for the search algorithm: [(integrin) OR (angiogenesis) OR (RGD) OR (NODAGA)] AND [(PET) OR (positron)] AND ((myocard*) OR (cardi*) OR (heart) OR (cardiovascular) OR (CAD)). The search was carried out from inception to October 26, 2021. To expand the search, references of the retrieved articles were also screened for additional studies.

Study Selection

Original articles within the field of interest reporting the role of RGD-based PET agents in patients with cardiovascular diseases were eligible for inclusion. The exclusion criteria were as follow: (a) original preclinical studies in the field of interest; (b) articles outside of the field of interest of this review; (c) case reports and small case series (<5 patients); (d) review articles, comments, letters, editorials, and conference proceedings. No language or date restrictions were used. The titles and abstracts of the recovered articles were reviewed independently by two researchers (MD and GT) according to the inclusion and exclusion criteria. Articles which appeared evidently ineligible according to these eligibility criteria were rejected. The full-length version of the remaining articles was independently reviewed by two researchers (MD and GT) to evaluate their eligibility for inclusion. Any disagreements over articles eligibility were resolved by consensus.

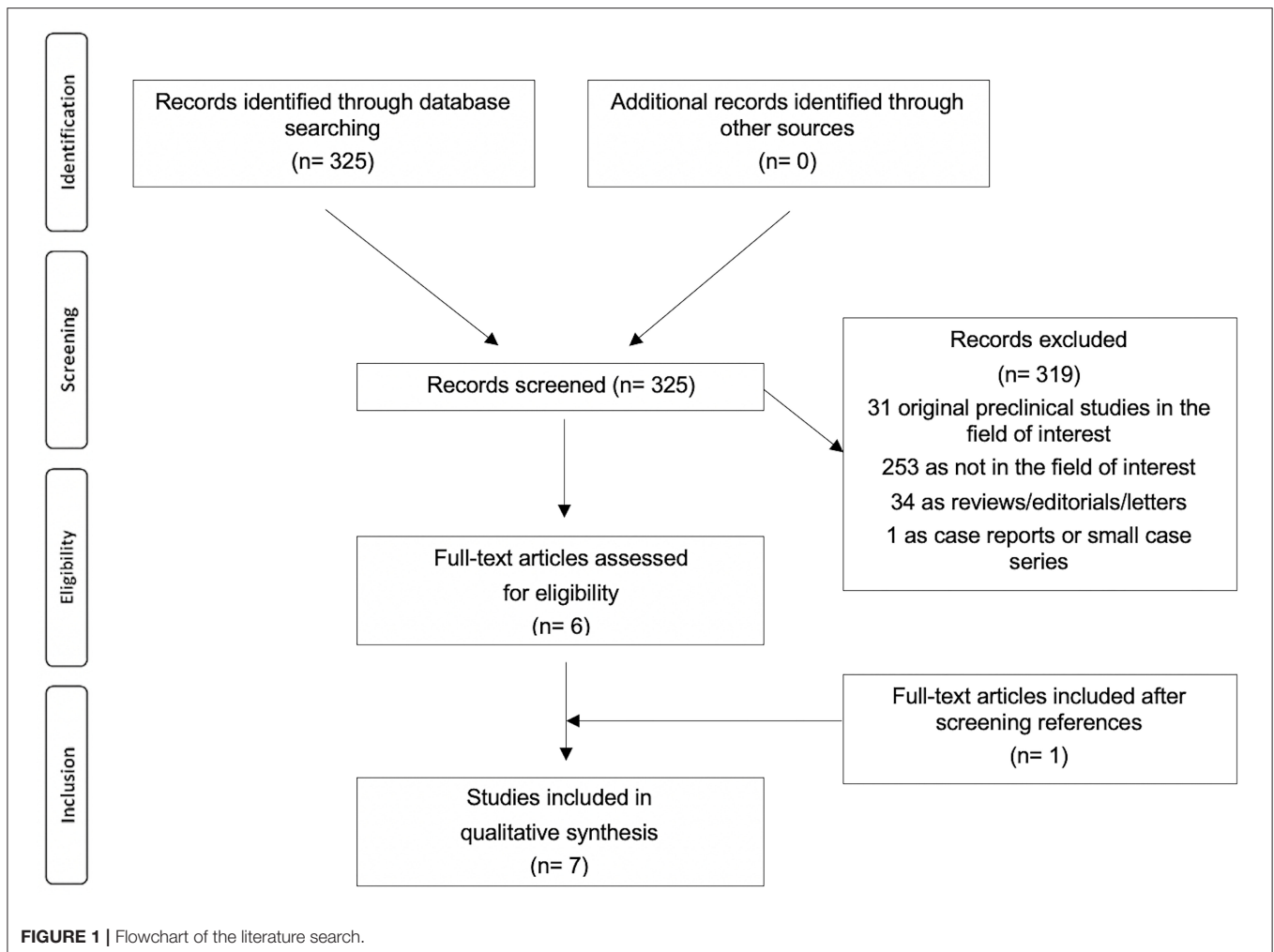
Quality Assessment

The quality assessment was performed according to the NIH Quality assessment tool for Observational Cohort and Cross-Sectional Studies (<https://www.nhlbi.nih.gov/health-topics/study-quality-assessment-tools>).

RESULTS

Literature Search

The review question was the role of RGD-based PET agents in patients with cardiovascular diseases. The literature search results using a systematic approach are reported in **Figure 1**. The comprehensive computer literature search from PubMed/MEDLINE and Cochrane library database revealed 325 records. Reviewing titles and abstracts, 319 records were excluded: 253 because they were not in the field of interest of this review; 34 reviews, editorials, letters, or comments; 31 preclinical studies, and 1 case report. Six articles were selected and retrieved in full-text version. One additional study was found screening the references of the selected articles. Finally, 7 articles (198 patients) including data on the role of RGD-based PET agents in patients with cardiovascular diseases were included in the systematic review (16–22). The characteristics of the studies selected for the systematic review are presented in **Tables 1–5**.



Qualitative Synthesis (Systematic Review) Basic Study and Patient Characteristics

Through the comprehensive computer literature search, 7 full-text articles including data on the role of RGD-based PET agents in patients with cardiovascular diseases were selected (Table 1) (16–22). All the selected articles were published in the last 9 years. Korea, the United Kingdom, China, Germany, and Switzerland were represented. All the studies were monocentric, 86% were prospective and 14% were retrospective. Two out of the seven studies (29%) focused only on the infarcted myocardium, one study focused on the infarcted myocardium and stroke (14%), one study focused only on stroke (14%), and the remaining 3 studies (43%) focused on atherosclerosis. Included patients had high rates of cardiovascular diseases: 130 out of the 198 patients (66%) had previous MI or stroke or were scheduled for carotid endarterectomy. The number of patients performing PET with RGD-based PET agents in cardiovascular studies ranged from 10 to 46. The mean age of the included patients ranged from 6.1 to 68.5 years; the female percentage was variable from 0 to 50%.

The quality of all the selected studies is judged as moderate according to the NIH quality assessment tools (see Supplementary Figure 1).

Technical Aspects

The included studies had heterogeneous technical aspects (Table 2). Five different radiotracers were used, the most frequent being ^{18}F -Galacto-RGD and ^{18}F -fluciclatide. The hybrid imaging modality was PET/CT for all the studies (no PET/MR study recorded). The radiopharmaceutical injected activity varied among the included studies (Table 2). The mean time interval between radiotracer injection and image acquisition varied among the included studies, from 20 to 120 min. Fasting was not requested before radiolabelled RGD-based injection. The PET image analysis was performed by using qualitative (visual) analysis and additional semi-quantitative analysis through the calculation of standardized uptake values (SUV) in most studies (6 out of the 7 studies: 86%). All reported values were corrected for mean radiotracer activities in the normal myocardium, and/or the normal brain, the blood, the liver, the most frequent being the blood pool activity.

TABLE 1 | Basic study and patient characteristics of the included studies.

References	Country	Study design	Study focus	Number of patients	MI patients	Stroke patients or patients scheduled for carotid endarterectomy	Average age (range)	Male/Female
Choi et al. (22)	Korea	Prospective	Stroke	10	NR	10	6.1 (2–14)*	5/5†
Sun et al. (16)	China	Prospective	MI	39	23	16	MI Patients: 61 (45–82) Stroke Patients: 56 (33–80)	30/9
Beer et al. (17)	Germany	Prospective	Atherosclerosis	10	NR	10	68.5 (55–79)	NR
Jenkins et al. (19)	United Kingdom	Prospective	MI	37	21	NR	64 ± 10 (NR)	27/10
Jenkins et al. (19)	United Kingdom	Prospective	Atherosclerosis	46	24	NR	66 ± 10 (NR)	34/12
Makowski et al. (20)	Germany	Prospective	MI	12	12	NR	53 ± 12 (NR)	12/0
Dietz et al. (21)	Switzerland	Retrospective	Atherosclerosis	44	5	5	60 (NR)	24/20

MI, myocardial infarction; NR, not reported.

*Age 1–14 years in the method section.

†Male/Female 6/4 in the method section.

Main Findings for Studies Focused on the Infarcted Myocardium

Twenty-nine out of the 56 (52%) MI patients in studies focused on the infarcted myocardium had ST-elevation MI (STEMI), 6 out of the 56 (11%) MI patients had non-ST-elevation MI (NSTEMI), and this information was not available in the 21 remaining patients (38%). The main outcome measurements of RGD-based tracer accumulation in the infarcted myocardium are listed in **Table 3** and include correlation between RGD uptake and MI size, characterization of RGD uptake pattern, histological correlates, and the temporal expression of RGD uptake. The time interval between MI and RGD-based PET/CT varied from 3 days to 2 years, most patients undergoing RGD-based PET/CT within 3 months after the MI attack. Importantly, 63 out of the 73 RGD-based PET acquisitions (86%) displayed positive radiotracer uptake in the infarcted zones. Other modalities used to outline the infarcted zones were ^{99m}Tc -MIBI, cardiac MRI and [^{13}N]NH $_3$ PET.

The MI size was determined by ^{99m}Tc -MIBI cardiac perfusion imaging (measurements of the maximum diameters of the infarcted regions), cardiac MRI (measurements in g/m^2) or [^{13}N]NH $_3$ perfusion PET (% of left ventricle). Two out of the three studies found correlation between RGD uptake and MI size but the remaining third study did not find any correlation.

Concerning the correlation between perfusion and RGD uptake, Makowski et al. found a per-segment negative correlation between tracer uptake of [^{18}F]Galacto-RGD and blood flow, as measured by [^{13}N]NH $_3$ (20). Interestingly, Sun et al. found ^{68}Ga -PRGD2 uptake to be located at or immediately around the area of infarction outlined by matched ^{99m}Tc -MIBI perfusion images and ^{18}F -FDG metabolism images (16). This finding supports a potential increased $\alpha_v\beta_3$ expression also in non-viable tissue, as defined by regional reductions in ^{18}F -FDG uptake in proportion to regional reductions in myocardial perfusion.

Only 1 out of the 3 studies reported histopathological analysis in an exploratory analysis for two patients, finding positive staining for $\alpha_v\beta_3$ integrin, largely in regions that co-localized to vascular endothelial cells. Lower numbers of CD68-positive inflammatory cells and smooth muscle actin-positive myofibroblasts co-registered also with $\alpha_v\beta_3$ integrin expression were found in their exploratory analysis (18). One out of the 3 studies studied the temporal expression of the RGD uptake using serial assessments, with 17 out of the 21 patients agreeing to return for a second RGD PET/CT 76 ± 19 days post-MI and found a reduced RGD uptake intensity as compared with earlier imaging 14 ± 7 days post-MI (18).

The study from Jenkins et al. was also the only study that assessed the correlation between RGD uptake and functional recovery. Interestingly, they found an association between increased $\alpha_v\beta_3$ expression and improvement of wall motion (18).

A representative example of RGD PET/CT imaging in the infarcted myocardium is illustrated in **Figure 2**.

Main Findings for Studies Focused on Atherosclerosis

The arterial segments assessed were internal and common carotid arteries, ascending aorta, aortic arch, descending aorta,

TABLE 2 | Technical aspects of RGD-based PET/CT in the included studies.

References	PET/CT scanner	Tracers used	Mean injected activity (range)	Mean time interval between radiotracer injection and image acquisition	PET/CT image analysis	
					Semi-quantitative	Reference
Choi et al. (22)	NR	⁶⁸ Ga-NOTA-RGD	111	20 min	Lesion to control ratios	Normal brain
Sun et al. (16)	Siemens Biograph 64 TruepointTrueV	⁶⁸ Ga-NOTA-PRGD2	1.85 MBq/kg	30 min	SUV _{peak} ; SUV ratios	Normal myocardium; normal brain
Beer et al. (17)	Siemens Biograph Sensation 16	¹⁸ F-Galacto-RGD	188 ± 16 (NR) MBq	90 min	SUV _{mean} ; TBR	Common carotid artery
Jenkins et al. (19)	Siemens Biograph mCT	¹⁸ F-fluciclatide	229 ± 12 (NR) MBq	40 min	SUV _{mean} ; SUV _{max} ; TBR	Superior vena cava
Jenkins et al. (19)	Siemens Biograph mCT	¹⁸ F-fluciclatide	229 (NR) MBq	40 min	SUV _{mean} ; SUV _{max} ; TBR	Superior vena cava
Makowski et al. (20)	Siemens Biograph Sensation 16	¹⁸ F-Galacto-RGD	188 ± 19 (NR) MBq	120 min	SUVs; SUV ratios	Normal myocardium, blood, liver
Dietz et al. (21)	GE Discovery 690 TOF; Siemens Biograph Vision 600	⁶⁸ Ga-NODAGA-RGD	190 (NR) MBq	63 min	SUV _{max} ; SUV _{mean} ; TBR	Inferior and superior vena cava

NR, not reported; SUV, standardized uptake value; TBR, target-to-background ratio.

abdominal aorta, and iliac arteries. One study focused only on internal and common carotid arteries and another study focused only on thoracic aorta for *in vivo* imaging (17, 19). No study assessed the coronary arteries. The main outcome measurements of RGD-based tracer accumulation in atherosclerosis are listed in **Table 4** and include clinical, morphological, and histological correlates. The median intensity of tracer uptake as determined by TBR measurements ranged from 1.31 (IQR 1.62–2.04) to 1.84 (IQR 1.62–2.04), but these data were available only in 2 out of 3 studies (19, 21). Only one study included a binary visual analysis and found a positive signal in carotid plaques on PET using ⁶⁸Ga-NOTA-PRGD2 in only half of the patients (5 out of 10 patients) (17).

Two studies focused on clinical correlates and found correlation with prior cardiovascular or cerebrovascular events as well as with history of hypercholesterolemia (19, 21).

Morphological imaging was included in all studies. Two studies focused on CT plaque burden in large vessels and found correlation with CT calcium scoring and/or the indexed plaque volume (19, 21). One study included further exploration using ultrasound and MR angiography and found a higher tracer accumulation in areas of the carotids with medium- or high-grade stenosis compared with areas with none/low-grade stenosis (17).

Finally, 2 out of the 3 studies reported histopathological analysis and found a co-localization between tracer accumulation and areas of $\alpha_v\beta_3$ expression (17, 19).

A representative example of RGD PET/CT imaging in atherosclerosis is illustrated in **Figure 3**.

Main Findings for Studies Focused on Stroke

The stroke symptoms were described as hemiplegia, hemidysesthesia and/or hemianopsia in the 16 stroke patients included in the study from Sun et al. (16) and were not described in the 10 stroke patients included in the study from Choi et al. (22). The main outcome measures about the RGD-based tracer accumulation in cerebral infarct are listed in **Table 5** and include correlation between RGD uptake and stroke size, characterization of RGD uptake pattern, and the temporal expression of RGD. The time interval between the event and RGD-based PET/CT varied from 1 day to 4 years, with most patients within 1 month after the cerebral attack. On a per-lesion analysis, 16 out of the 33 cerebral infarct zones (48%) displayed positive radiotracer uptake. Seventeen out of the thirty-three cerebral infarct zones (52%) were negative. Other modalities used to determine the infarct zones were ^{99m}Tc-HMPAO, brain MRI and ¹⁸F-FDG PET/CT. Only one study studied the correlation between RGD uptake and stroke size, measured over the CT images by referring to the ¹⁸F-FDG images (16). They found a positive correlation between RGD uptake and infarct size in a limited number of patients ($n = 10$) scanned 13–26 days after the event (**Table 5**). However, the authors pointed out two patients scanned 4 days after the event with mildly elevated RGD uptake despite relatively large low-density stroke regions on CT (SUV_{peak} = 0.15 and 0.16, maximum diameters 69.8 and 101.3 mm, respectively). No other data about the correlation between RGD uptake and stroke size was reported. This same study described the uptake pattern as a punctate multifocal form, mainly along the surrounding blood vessels (16). These authors also assessed the temporal expression of the RGD uptake using serial assessments with repeated scans at 3 months post event,

TABLE 3 | Summary of PET findings for studies focused on the infarcted myocardium.

References	MI type	RGD-based tracer accumulation				RGD-based tracer changes according to time after the event	Correlation between RGD uptake and MI size	Other modalities used to determine the infarcted zones	Uptake pattern	Histological correlates
		Days after MI	Positive number	SUV values	Negative number					
Sun et al. (16)	NR (one NSTEMI patient specified among the negative patients)	3 days–2 years	20/23	SUV _{peak} 1.94 ± 0.48, SUV ratios 2.33 ± 1.04, with peak uptake 1 week after MI	3	No serial assessment. Peak uptake 1 week after MI. Plateau within 4–75 days after MI	Yes ($r = 0.748$, $P = 0.001$)	^{99m} Tc-MIBI/cardiac ¹⁸ F-FDG PET/CT	Patchy form, within the area of infarction or immediately around	NR
Jenkins et al. (19)	STEMI	14 ± 7 days ($n = 21$)	21	TBR _{mean} 1.34 ± 0.22	0	Reduced intensity on second PET/CT scans	No ($r = 0.03$, $P = 0.90$)	Cardiac MRI	Within the area of infarction	Viable myocardium with widespread positive staining for $\alpha_v\beta_3$ integrin (exploratory analysis for two patients)
		76 ± 19 days ($n = 17$)	17	TBR _{mean} 1.20 ± 0.21	0					
Makowski et al. (20)	7 STEMI/5 NSTEMI	31 ± 14 days	5	Lesion/blood 1.15 ± 0.06; lesion/liver 0.61 ± 0.18	7	NR	Yes (moderate, $r = 0.73$, $P = 0.016$)	Cardiac MRI/[¹³ N]NH ₃ PET	Within the area of infarction or immediately around	NR

NR, not reported; MI, myocardial infarction; STEMI, ST-elevation myocardial infarction; NSTEMI, Non-ST-elevation myocardial infarction.
 r = Pearson correlation analysis.

TABLE 4 | Summary of PET findings for studies focused on atherosclerosis.

References	Arterial segment	RGD-based tracer accumulation			Clinical correlates	Morphological imaging correlates	Histological correlates
		Values; median (IQR)	Positive number	Negative number			
Beer et al. (17)	Internal and common carotid arteries	NR	In 5 patients (50%)	In 5 patients (50%)	NR	Higher tracer accumulation in areas of the carotids with medium- or high-grade stenosis compared with areas with none/low-grade stenosis (stenosis classified by using ultrasound and MR angiography, $P = 0.04$).	$\alpha_v\beta_3$ expression ($r = 0.787$, $P = 0.026$)
Jenkins et al. (19)	Ascending aorta, aortic arch, and descending thoracic aorta (for <i>in vivo</i> imaging)	SUV _{mean} 2.73 (2.35–3.05) SUV _{max} 3.65 (3.04–4.01) TBR 1.31 (1.20–1.39)	NR	NR	Higher tracer accumulation in patients with recent MI ($P = 0.02$), with hypercholesterolaemia ($P = 0.01$) and with established ischemic heart disease ($P = 0.04$)	CT plaque burden ($r = 0.37$, $P = 0.01$), mean wall thickness ($r = 0.57$, $P < 0.001$), and plaque volume ($r = 0.56$, $P < 0.001$) recorded on CT	Tracer accumulation co-localized with areas of $\alpha_v\beta_3$ expression, angiogenic endothelial cells, and inflammatory macrophages (in four human carotid intimal samples)
Dietz et al. (21)	Common carotid arteries, ascending aorta, aortic arch, descending aorta, abdominal aorta, and iliac arteries	TBR 1.84 (1.62–2.04)	NR	NR	Higher tracer accumulation in patients with previous clinically documented atherosclerotic cardiovascular disease ($P = 0.001$). Positive correlation with prior cardiovascular or cerebrovascular event ($r = 0.33$, $P = 0.027$), BMI ($\rho = 0.38$, $P = 0.01$), and history of hypercholesterolemia ($r = 0.31$, $P = 0.04$).	CT plaque burden ($\rho = 0.31$, $P = 0.04$)	NR

NR, not reported.

r = Pearson correlation analysis.

ρ = Spearman correlation analysis.

TABLE 5 | Summary of PET findings for studies focused on stroke.

References	Explicit neurologic symptoms	RGD-based tracer accumulation		RGD-based tracer changes according to time after the event	Correlation between RGD uptake and stroke size	Other modalities used to determine the infarct zones	Uptake pattern	Histological correlates
		Days after the event	Positive number					
Choi et al. (22)	13/17 (per lesion analysis)	1–422 days	8/17 (per lesion analysis)	No SUV value reported, lesion to control ratios 3.9±4.09	NR	Brain MRI/ ⁶⁸ mTc-HMPAO perfusion	Higher tracer accumulation in the three lesions with hyperperfusion as compared with the other lesions (<i>P</i> = 0.033)	NR
Sun et al. (16)	16/16 patients	4–13 years (<i>n</i> = 16)	8/16	SUV _{peak} 0.46 ± 0.29, SUV ratios 3.29 ± 1.09, with peak uptake 2 weeks after the event	In patients scanned 13th–26 days after the event (<i>r</i> = 0.835, <i>P</i> = 0.003)	Brain MRI/brain ¹⁸ F-FDG PET/CT	Punctate multifocal form	NR
		3 months (<i>n</i> = 2)	1/2	SUV _{peak} 0.16 (<i>n</i> = 1)		Brain ¹⁸ F-FDG PET/CT		

NR, not reported.

but with a very limited number of patients (*n* = 2). They found a reduced intensity (*n* = 1) or disappearance (*n* = 1) on second PET/CT scans.

DISCUSSION

Since the first successful clinical applications of an RGD PET radiopharmaceutical two decades ago, all the final eligible articles included in this review (*n* = 7) were published in the last 9 years, reflecting a recent growing interest in RGD PET/CT imaging focused on cardiovascular diseases (16–22). These studies varied in size and methodology. Two main topics can be distinguished: the infarcted myocardium and atherosclerosis. Stroke is a third topic that can be distinguished, but slightly less studied. All studies had a relatively clearly stated, clinically relevant, and patient-related purpose. Longitudinal studies that tell more about the natural history of $\alpha_v\beta_3$ expression in cardiovascular diseases using PET imaging were in very short supply. Interventional studies or randomized controlled trials have not been conducted so far. Due to this diversity, our systematic review could not provide an answer to a particular scientific question; we were left to summarize the main information about RGD PET in cardiovascular diseases that the literature had provided until now and point to some major issues that remain unanswered.

Infarcted Myocardium and $\alpha_v\beta_3$ Integrin Expression

Ventricular remodeling defines the changes that occur in structure, geometry, and function of the myocardium after MI. This biological process involves inflammation, angiogenesis, repair, and healing with specific biochemical and structural alterations in the infarcted myocardium, peri infarcted and remote regions. Several cell populations are involved, such as neutrophils, monocytes/macrophages, fibroblasts, T cells, stem cells, etc. (23, 24). Understanding reparative mechanisms following MI is becoming increasingly important. In some circumstances, maladaptive persistent processes may be detrimental. This may encourage remodeling and scarring to extend into the myocardium long after the initial causative injury, leading to progressive ventricular dilatation, ventricular dysfunction, and heart failure (25, 26).

The expression of $\alpha_v\beta_3$ integrin following MI, using PET imaging technique, could be of great interest. In contrast to a low level of expression by quiescent endothelial cells, $\alpha_v\beta_3$ integrin was found to be upregulated in state of angiogenesis within the myocardium after infarction in preclinical studies in rats (13, 14). $\alpha_v\beta_3$ integrin expression was also documented by both activated cardiac myofibroblasts and macrophages during margination and chemotaxis. Thus, $\alpha_v\beta_3$ integrin expression could play a central role in the coordination of the repair processes following MI.

Prevalence and Natural History of RGD PET Uptake in the Infarcted Myocardium, and Future Potential Directions

Forty-six out of the 56 (90%) MI patients in PET studies focused on the infarcted myocardium presented RGD uptake in the

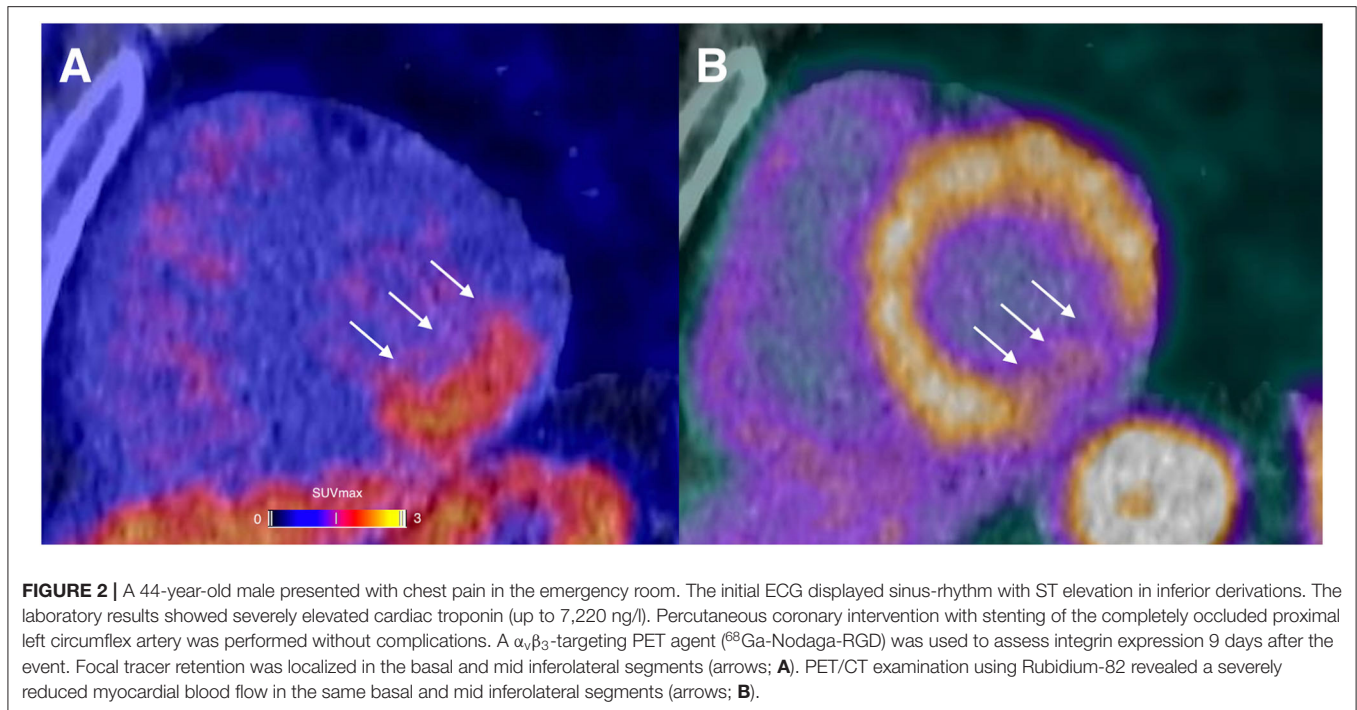


FIGURE 2 | A 44-year-old male presented with chest pain in the emergency room. The initial ECG displayed sinus-rhythm with ST elevation in inferior derivations. The laboratory results showed severely elevated cardiac troponin (up to 7,220 ng/l). Percutaneous coronary intervention with stenting of the completely occluded proximal left circumflex artery was performed without complications. A $\alpha_v\beta_3$ -targeting PET agent (^{68}Ga -Nodaga-RGD) was used to assess integrin expression 9 days after the event. Focal tracer retention was localized in the basal and mid inferolateral segments (arrows; **A**). PET/CT examination using Rubidium-82 revealed a severely reduced myocardial blood flow in the same basal and mid inferolateral segments (arrows; **B**).

infarcted area, demonstrating that $\alpha_v\beta_3$ integrin expression in the infarcted myocardium is well evident in RGD PET/CT scans.

In human studies of acute MI, RGD-based PET radiotracers accumulate at the site of infarction as early as 3 days and seem to be peaking at 1–3 weeks post-MI before being decreasing (16, 18). However, only one study assessed serial changes of myocardial RGD uptake after ischemic intervention (18). Moreover, the timepoint of the second ^{18}F -fluciclatide PET/CT after MI in this single study was particularly variable (76 ± 19 days). Changes of myocardial RGD PET uptake in humans after coronary occlusion and reperfusion is still to be precisely determined. Serial changes of myocardial RGD PET uptake are studied in more detail in an ongoing prospective study (ClinicalTrials.gov NCT03809689).

Vessel damage with ischemic insult is expected to occur during the first days after MI (27, 28), which could lead to unspecific tracer diffusion in damaged leaky vessels. Here, the peak of tracer accumulation at 1–3 weeks post-MI is in favor of minimal effects of this unspecific tracer diffusion in damaged leaky vessels. Myocardial uptake post MI using RGD PET/CT may thus be predominantly due to integrin expression rather than unspecific leakage. However, no imaging was performed at day 1 in the different studies.

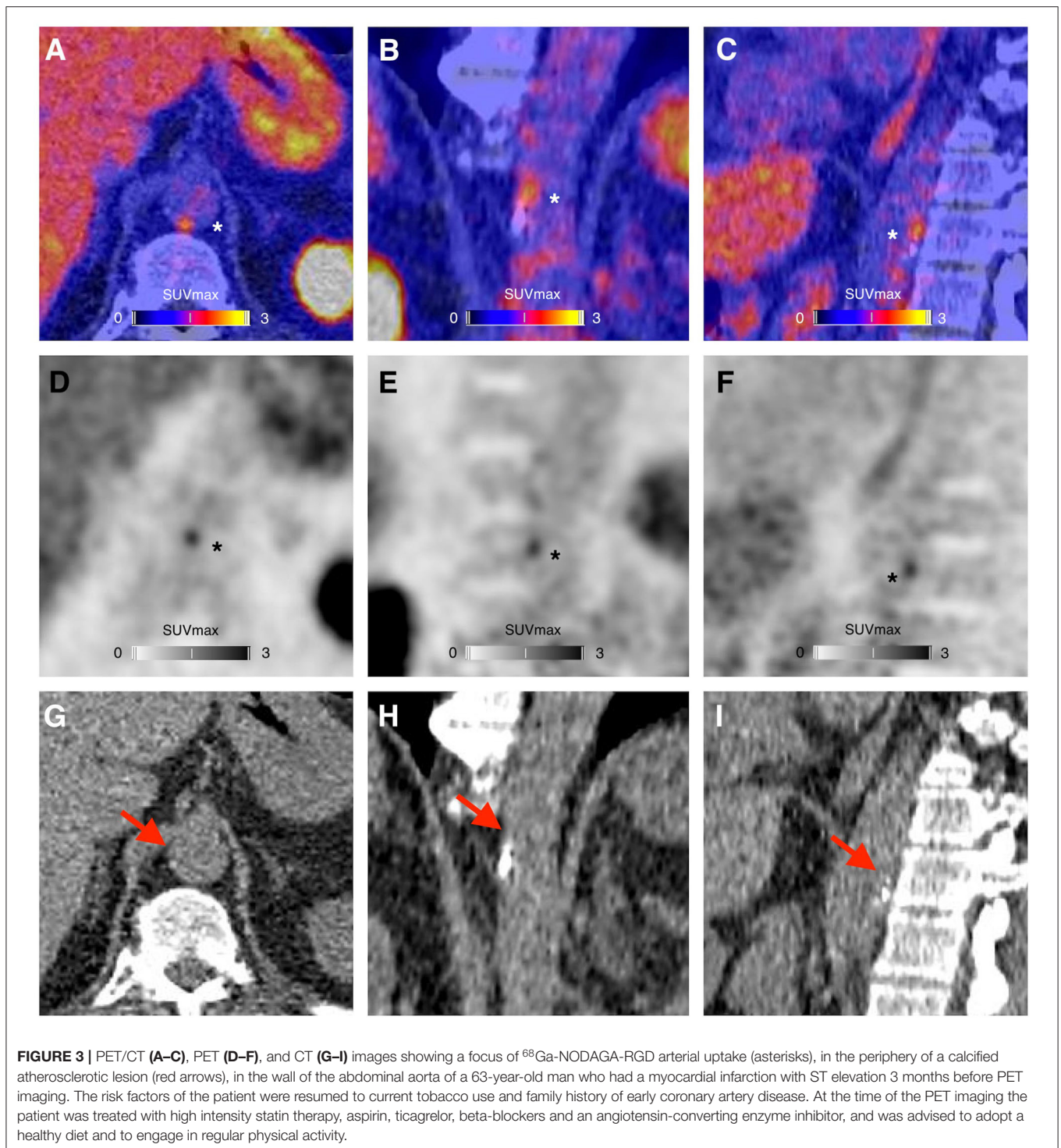
An interesting finding in both studies from Sun et al. (16) and Jenkins et al. (18) was the absence of increase in RGD uptake in chronically damaged myocardium, indicating minimal residual $\alpha_v\beta_3$ integrin expression in old ischemic injuries. Therefore, $\alpha_v\beta_3$ integrin expression seems rather to act as a marker of cardiac repair at sites of recent MI (16, 18).

Despite those promising results further prospective studies are nevertheless warranted to confirm a clinical value of RGD PET uptake as a prognostic marker for left ventricular remodeling.

Moreover, some findings support increased $\alpha_v\beta_3$ expression also in non-viable tissue, which could be explain by a linking to the myofibroblasts (16, 29). Studies assessing the prognostic value of RGD PET uptake in the infarcted myocardium are still needed.

Atherosclerosis and $\alpha_v\beta_3$ Integrin Expression

The ability to accurately and non-invasively monitor inflammatory processes in atherosclerotic plaques would represent a major advance, and metabolic imaging using PET has the potential to fulfill this important unmet clinical need. Integrin $\alpha_v\beta_3$ has been widely studied in atherosclerosis. In the development of atherosclerosis, expression of integrin $\alpha_v\beta_3$ has been found in endothelial cells as well as in CD68-positive macrophages, and both inflammation and angiogenesis processes are associated with plaque growth, plaque instability and clinical events (10–12). The necrotic core in the culprit plaque results from increasing inflammation (30). Pro-atherogenic stimuli lead to an infiltration of activated monocytes within the intima, which differentiate into pro-inflammatory macrophages (31). The apoptosis of the resident pro-inflammatory macrophages leads to the development of a lipid-rich or necrotic core (30). Matrix metalloproteinases secreted by macrophages weaken the fibrous cap, predisposing it to rupture. Angiogenesis is believed to occur in response to hypoxic conditions within the necrotic core. Neovessels, arising from the adventitial vasa vasorum, grow into the base of progressive atherosclerotic lesions and provide an alternative entry pathway for monocytes and immune cells. The plaque neovessels are fragile and leaky, giving rise to local extravasation of plasma proteins and erythrocytes (32). Plaque



hemorrhage itself results in a pro-inflammatory response, plaque destabilization and clinical events (11, 33).

Attractive Promising Results of RGD-Based PET Agents in Atherosclerosis

Overall, although the numbers are limited, the existing studies support the potential of RGD-based PET imaging of $\alpha_v\beta_3$

integrin expression in atherosclerosis. ^{18}F -fluciclatide PET/CT has proven itself as a potential valuable target for the imaging of unstable atherosclerosis (19). ^{68}Ga -NODAGA-RGD uptake in large vessels showed clinical correlation with atherosclerotic cardiovascular diseases (21). ^{18}F -Galacto-RGD PET/CT showed specific tracer accumulation in human atherosclerotic carotid plaques, with increased PET signals observed in stenotic compared with non-stenotic areas based on MR or CT

angiography data, and with histological correlation with $\alpha_v\beta_3$ expression (17).

Intensity of RGD PET Uptake in Plaque Imaging in Humans

Background corrections were systematically used among different studies. Again, the median intensity of arterial tracer uptake as determined by TBR measurements were 1.31 (IQR 1.20–1.39) for the study from Jenkins et al. (19) and 1.84 (IQR 1.62–2.04) for the study from Dietz et al. (21). Interestingly, Dietz et al. used a SiPM PET system (Biograph Vision 600, Siemens Medical Solutions, Knoxville, USA) in 16 out of 44 (36%) of the patients included for the analysis, which could partly explain the highest TBR measurements. SiPM PET is a new PET technology with improved spatial and timing resolution and a relatively high sensitivity and count-rate capability as compared to PET scanners using conventional photomultiplier tubes (34).

The TBR measurements were slightly lower than those of other established tracers used for plaque imaging. In a study using ^{18}F -sodium fluoride for visualization of microcalcification in plaque in the major arteries, the mean TBR was 2.3 ± 0.7 (35). In another study using ^{68}Ga -Pentixafor for visualization of inflammatory cells, the mean TBR was 2.0 ± 0.5 (36).

The difference in intensity of TBR between non-calcified/mixed/calcified plaques on CT has not been studied so far. However, Dietz et al. found that only around 26% of ^{68}Ga -NODAGA-RGD highest uptake foci in their cohort were colocalized to calcification on CT (21). This result suggests that RGD accumulation could particularly occur mainly in the non-calcified vessel wall, which may indicate some association with pathophysiologic processes found in early atherosclerotic disease.

Future Potential Directions of $\alpha_v\beta_3$ Integrin Expression in Plaque Imaging

To date, RGD PET imaging in humans has emerged as a promising tool for the assessment of active atherosclerosis processes, but with a still very limited number of studies ($n = 3$) (17, 19, 21). All studies were focused on subjects with established disease, and there is no work which has investigated whether RGD uptake could predict future events or whether it can provide additional prognostic information over current methods of risk stratification. Further works are also needed to establish whether RGD PET could monitor disease progression, guide therapeutic interventions, or assess novel anti-angiogenic therapies in cardiovascular diseases.

It is also not well established whether having a recent MI would lead to a significant increase in aortic plaque microvessels, or indeed whether these changes are likely to occur within 1–3 weeks post MI. Because integrins $\alpha_v\beta_3$ are expressed in neovessels in plaques but also in CD68-positive macrophages, it is not possible to ascertain with PET only whether RGD is binding preferentially to one or the other of these processes. Aortic RGD uptake post MI in large vessels could be reporting predominantly on systemic inflammation rather than microvessels proliferation (37).

No study assessed the coronary arteries. The potential value of integrin tracers would be of great interest for future trials, as most PET tracers are not suitable due to too low signal for coronary artery disease assessment. Moreover, the capacity of the paradigm based on ischemia to prevent MI is increasingly being questioned, and the quantification of metabolic activity of atherosclerotic disease is of growing interest (38). PET imaging with integrin tracers could have the potential to add value to this purpose.

No PET study in humans assessed $\alpha_v\beta_3$ integrin expression in aortic aneurysm, which could be of clinical interest. Degraded aortic tissue is known to exhibit abnormal angiogenesis and is present in abundance at sites of aortic rupture (39). $\alpha_v\beta_3$ integrin expression stimulate angiogenesis, typically in hypoxic environments (40). The predictive value of $\alpha_v\beta_3$ integrin expression imaging using PET in aortopathy to predict disease progression is unknown.

RGD PET Uptake in Stroke

PET studies focused on ischemic cerebral vascular disease are scarce ($n = 2$) (16, 22). As in the normal myocardium, the PET RGD-peptide was absent in the normal brain, allowing a clear background to evaluate the post-stroke angiogenesis. However, the RGD PET uptake levels in stroke seem to be lower than those in MI (16). These could indicate difficulties of forming new capillaries from the pre-existing vessels after stroke (16). The existing data support that $\alpha_v\beta_3$ integrin expression in the cerebral infarct is prominent in the acute phase (<30 days after the event) and decrease with time, but evidence is still lacking. Serial changes of cerebral RGD uptake were assessed for only two patients (16). However, both existing studies have consistent findings in chronically damaged brain, with absent or very weak uptake reported.

Some evidence supports a strong correlation between RGD uptake and stroke size but only in a limited number of patients scanned 13–26 days after the event (16). Like in MI, a non-perfect correlation between RGD uptake and standard measures of infarct severity like the infarct size could suggest that RGD uptake is not a surrogate of infarction but could relate more to the tissue-healing response to injury.

An interesting finding in the study from Sun et al. is a punctate multifocal RGD uptake along the surrounding blood vessels in stroke patients, contrasting with the patchy-form uptake found in MI patients (16). The authors explained that the myocardial remodeling could contribute to this different uptake pattern, but more data are needed to confirm these findings.

Radiolabeling of RGD-Based PET Agents

Most of the RGD-based radiotracers included in this systematic review were labeled with ^{18}F (4 out of the 7 studies: 57%). The remaining 2 out of the 7 studies (29%) used RGD-based radiotracers labeled with ^{68}Ga obtained from a $^{68}\text{Ge}/^{68}\text{Ga}$ generator. Imaging relatively thick structure like the left ventricle is not an issue using PET imaging but the use of ^{18}F labeled tracers for atherosclerotic PET imaging could have several physical and technical advantages as compared to ^{68}Ga labeled tracers. In fact, ^{68}Ga has higher positron energy and positron range which could lead to noisier images and worse spatial

resolution, which could be amplified by a lower injected activity of ^{68}Ga compared with ^{18}F (at least using traditional photomultiplier tube PET/CT). However, the synthesis of ^{18}F -Galacto-RGD tracer used by Beer et al. could be complex and time consuming, making an automated production process, which is mandatory for routine clinical use, extremely difficult (17, 41, 42). Moreover, ^{68}Ga labeled tracers have already been extensively used to image atherosclerotic plaques in large vessels, and in vessels as small as the coronary arteries (36, 43, 44). The superiority of a labeling with ^{18}F or ^{68}Ga is not clear for RGD-based radiotracers for cardiovascular PET imaging.

Limitations

We should report several limitations in our systematic review, which could limit the scope of our results. Our eligibility criteria lead to a very small number of original articles eligible for inclusion in this systematic review, with limited histological assessment. This systematic review focused on PET, and studies focusing on SPECT were not included. Unlike SPECT imaging, PET imaging does not require an extrinsic collimator resulting in higher count sensitivity and spatial resolution. Moreover, accurate and well validated attenuation correction is available with PET. This provides routinely available quantitative assessments (45), which could be crucial. In fact, important potential clinical applications of molecular integrin imaging in cardiovascular diseases could provide quantitative endpoints for use in clinical trials.

There was significant heterogeneity across the studies in terms of technical aspects. Different radiotracers were used. The radiopharmaceutical injected activity and the mean time interval between radiotracer injection and image acquisition varied among the included studies.

For atherosclerosis imaging, it cannot be ruled out that tracer signals observed with RGD PET are at least partially attributable to noise, especially using ^{68}Ga labeling (46).

Finally, despite a high number of prospective studies with relatively clearly stated and patient-related purposes, according to the NIH quality assessment tool the quality of the seven selected studies is judged as moderate, mainly as they were single center and with a limited number of patients. We have tried to minimize publication bias

excluding case reports or small case series from this systematic review.

CONCLUSIONS

From this systematic review on the role of RGD-based PET agents in patients with cardiovascular diseases, we are led to conclude that data on PET imaging of integrin $\alpha_v\beta_3$ in patients with cardiovascular diseases are still very limited. PET imaging can provide insight on unique markers of disease activity, such as neoangiogenesis and inflammation, which are crucial to the pathogenesis of cardiovascular diseases. Promising applications using RGD-based PET agents are emerging, such as prediction of remodeling processes in the infarcted myocardium or detection of active atherosclerosis, with potentially significant clinical impact.

DATA AVAILABILITY STATEMENT

The raw data supporting the conclusions of this article will be made available by the authors, without undue reservation.

AUTHOR CONTRIBUTIONS

MD and GT: conceptualization and investigation. GT: methodology. MD: writing—original draft preparation. MD, CK, VD, SF, VR, NT, AS, MJ, SB, MN, NS, NM, JP, and GT: writing—review and editing. JP and GT: supervision. All authors have read and agreed to the published version of the manuscript.

FUNDING

MD was supported by Research Fellowship Awards from the Société Française de Radiologie, Paris, France, and from the Agence Régionale de Santé Auvergne-Rhône-Alpes, Lyon, France. Open access funding was provided by the University of Lausanne.

SUPPLEMENTARY MATERIAL

The Supplementary Material for this article can be found online at: <https://www.frontiersin.org/articles/10.3389/fmed.2022.887508/full#supplementary-material>

REFERENCES

- Dagenais GR, Leong DP, Rangarajan S, Lanas F, Lopez-Jaramillo P, Gupta R, et al. Variations in common diseases, hospital admissions, and deaths in middle-aged adults in 21 countries from five continents (PURE): a prospective cohort study. *Lancet*. (2020) 395:785–94. doi: 10.1016/S0140-6736(19)32007-0
- Pierschbacher MD, Ruoslahti E. Cell attachment activity of fibronectin can be duplicated by small synthetic fragments of the molecule. *Nature*. (1984) 309:30–3. doi: 10.1038/309030a0
- Aumailley M, Gurrath M, Müller G, Calvete J, Timpl R, Kessler H. Arg-gly-asp constrained within cyclic pentapeptides—strong and selective inhibitors of cell-adhesion to vitronectin and laminin fragment-P1. *FEBS Lett*. (1991) 291:50–4. doi: 10.1016/0014-5793(91)81101-D
- Brooks PC, Clark RAF, Cheresh DA. Requirement of vascular integrin $\alpha_v\beta_3$ for angiogenesis. *Science*. (1994) 264:569–71. doi: 10.1126/science.7512751
- Beer AJ, Haubner R, Göbel M, Luderschmidt S, Spilker ME, Wester HJ, et al. Biodistribution and pharmacokinetics of the $\alpha_v\beta_3$ -selective tracer ^{18}F -galacto-RGD in cancer patients. *J Nucl Med*. (2005) 46:1333–41.
- Beer AJ, Haubner R, Sarbia M, Göbel M, Luderschmidt S, Grosu AL, et al. Positron emission tomography using ^{18}F -Galacto-RGD identifies the level of integrin $\alpha_v\beta_3$ expression in man. *Clin Cancer Res*. (2006) 12:3942–9. doi: 10.1158/1078-0432.CCR-06-0266

7. Chen H, Niu G, Wu H, Chen X. Clinical application of radiolabeled RGD peptides for PET imaging of integrin $\alpha v \beta 3$. *Theranostics*. (2016) 6:78–92. doi: 10.7150/thno.13242
8. Steiger K, Quigley NG, Groll T, Richter F, Zierke MA, Beer AJ, et al. There is a world beyond $\alpha v \beta 3$ -integrin: multimeric ligands for imaging of the integrin subtypes $\alpha v \beta 6$, $\alpha v \beta 8$, $\alpha v \beta 3$, and $\alpha 5 \beta 1$ by positron emission tomography. *EJNMMI Res*. (2021) 11:106. doi: 10.1186/s13550-021-00842-2
9. Ebenhan T, Kleynhans J, Zeevaert JR, Jeong JM, Sathekge M. Non-oncological applications of RGD-based single-photon emission tomography and positron emission tomography agents. *Eur J Nucl Med Mol Imaging*. (2021) 48:1414–33. doi: 10.1007/s00259-020-04975-9
10. Hoshiga M, Alpers CE, Smith LL, Giachelli CM, Schwartz SM. Alpha-v beta-3 integrin expression in normal and atherosclerotic artery. *Circ Res*. (1995) 77:1129–35. doi: 10.1161/01.RES.77.6.1129
11. Virmani R, Kolodgie FD, Burke AP, Finn AV, Gold HK, Tulenko TN, et al. Atherosclerotic plaque progression and vulnerability to rupture: angiogenesis as a source of intraplaque hemorrhage. *Arterioscler Thromb Vasc Biol*. (2005) 25:2054–61. doi: 10.1161/01.ATV.0000178991.71605.18
12. Kolodgie FD, Gold HK, Burke AP, Fowler DR, Kruth HS, Weber DK, et al. Intraplaque hemorrhage and progression of coronary atheroma. *N Engl J Med*. (2003) 349:2316–25. doi: 10.1056/NEJMoa035655
13. Meoli DF, Sadeghi MM, Krassilnikova S, Bourk BN, Giardino FJ, Dione DP. Noninvasive imaging of myocardial angiogenesis following experimental myocardial infarction. *J Clin Invest*. (2004) 113:1684–91. doi: 10.1172/JCI200420352
14. Higuchi T, Bengel FM, Seidl S, Watzlowik P, Kessler H, Hegenloh R, et al. Assessment of v 3 integrin expression after myocardial infarction by positron emission tomography. *Cardiovasc Res*. (2008) 78:395–403. doi: 10.1093/cvr/cvn033
15. Page MJ, McKenzie JE, Bossuyt PM, Boutron I, Hoffmann TC, Mulrow CD, et al. The PRISMA 2020 statement: an updated guideline for reporting systematic reviews. *Syst Rev*. (2021) 10:1–11. doi: 10.1136/bmj.n71
16. Sun Y, Zeng Y, Zhu Y, Feng F, Xu W, Wu C, et al. Application of (68)Ga-PRGD2 PET/CT for $\alpha v \beta 3$ -integrin imaging of myocardial infarction and stroke. *Theranostics*. (2014) 25:778–86. doi: 10.7150/thno.8809
17. Beer AJ, Pelisek J, Heider P, Saraste A, Reeps C, Metz S, et al. PET/CT imaging of integrin $\alpha v \beta 3$ expression in human carotid atherosclerosis. *JACC Cardiovasc Imaging*. (2014) 7:178–87. doi: 10.1016/j.jcmg.2013.12.003
18. Jenkins WS, Vesey AT, Stirrat C, Connell M, Lucatelli C, Neale A, et al. Cardiac $\alpha v \beta 3$ integrin expression following acute myocardial infarction in humans. *Heart*. (2017) 103:607–15. doi: 10.1136/heartjnl-2016-310115
19. Jenkins WS, Vesey AT, Vickers A, Neale A, Moles C, Connell M, et al. In vivo alpha-V beta-3 integrin expression in human aortic atherosclerosis. *Heart*. (2019) 105:1868–75. doi: 10.1136/heartjnl-2019-315103
20. Makowski MR, Rischpler C, Ebersberger U, Keithahn A, Kasel M, Hoffmann E, et al. Multiparametric PET and MRI of myocardial damage after myocardial infarction: correlation of integrin $\alpha v \beta 3$ expression and myocardial blood flow. *Eur J Nucl Med Mol Imaging*. (2021) 48:1070–80. doi: 10.1007/s00259-020-05034-z
21. Dietz M, Kamani CH, Deshayes E, Dunet V, Mitsakis P, Coukos G, et al. Imaging angiogenesis in atherosclerosis in large arteries with 68Ga-NODAGA-RGD PET/CT: relationship with clinical atherosclerotic cardiovascular disease. *EJNMMI Res*. (2021) 14:71. doi: 10.1186/s13550-021-00815-5
22. Choi H, Phi JH, Paeng JC, Kim SK, Lee YS, Jeong JM, et al. Imaging of integrin $\alpha(V)\beta(3)$ expression using (68)Ga-RGD positron emission tomography in pediatric cerebral infarct. *Mol Imaging*. (2013) 12:213–7. doi: 10.2310/7290.2012.00036
23. Sutton MG, Sharpe N. Left ventricular remodeling after myocardial infarction. *Pathophysiol Ther Circ*. (2000) 101:2981–8. doi: 10.1161/01.CIR.101.25.2981
24. Weber KT. Extracellular matrix remodeling in heart failure: a role for *de novo* angiotensin II generation. *Circulation*. (1997) 96:4065–82. doi: 10.1161/01.CIR.96.11.4065
25. Swirski FK, Nahrendorf M. Leukocyte behavior in atherosclerosis, myocardial infarction, heart failure. *Science*. (2013) 339:161–6. doi: 10.1126/science.1230719
26. Jung K, Kim P, Leuschner F, Gorbatov R, Kim JK, Ueno T, et al. Endoscopic time-lapse imaging of immune cells in infarcted mouse hearts. *Circ Res*. (2013) 112:891–9. doi: 10.1161/CIRCRESAHA.111.300484
27. Rochitte CE, Lima JA, Bluemke DA, Reeder SB, McVeigh ER, Furuta T, et al. Magnitude and time course of microvascular obstruction and tissue injury after acute myocardial infarction. *Circulation*. (1998) 98:1006–14. doi: 10.1161/01.CIR.98.10.1006
28. Fernández-Jiménez R, Galán-Arriola C, Sánchez-González J, Agüero J, López-Martín GJ, Gomez-Talavera S, et al. Effect of ischemia duration and protective interventions on the temporal dynamics of tissue composition after myocardial infarction. *Circ Res*. (2017) 121:439–50. doi: 10.1161/CIRCRESAHA.117.310901
29. van den Borne SW, Isobe S, Verjans JW, Petrov A, Lovhaug D, Li P, et al. Molecular imaging of interstitial alterations in remodeling myocardium after myocardial infarction. *J Am Coll Cardiol*. (2008) 52:2017–28. doi: 10.1016/j.jacc.2008.07.067
30. Bentzon JF, Otsuka F, Virmani R, Falk E. Mechanisms of plaque formation and rupture. *Circ Res*. (2014) 114:1852–66. doi: 10.1161/CIRCRESAHA.114.302721
31. Clinton SK, Underwood R, Hayes L, Sherman ML, Kufe DW, Libby P, et al. Macrophage colony-stimulating factor gene expression in vascular cells and in experimental and human atherosclerosis. *Am J Pathol*. (1992) 140:301–16.
32. Sluimer JC, Kolodgie FD, Bijmens AP, Maxfield K, Pacheco E, Kutys B, et al. Thin-walled microvessels in human coronary atherosclerotic plaques show incomplete endothelial junctions relevance of compromised structural integrity for intraplaque microvascular leakage. *J Am Coll Cardiol*. (2009) 53:1517–27. doi: 10.1016/j.jacc.2008.12.056
33. Moreno PR, Purushothaman KR, Fuster V, Echeverri D, Trusczyńska H, Sharma SK, et al. Plaque neovascularization is increased in ruptured atherosclerotic lesions of human aorta: implications for plaque vulnerability. *Circulation*. (2004) 110:2032–8. doi: 10.1161/01.CIR.0000143233.87854.23
34. Koenders SS, van Dalen JA, Jager PL, Knolles S, Timmer JR, Mouden M, et al. Value of SiPM PET in myocardial perfusion imaging using Rubidium-82. *J Nucl Cardiol*. (2022) 29:204–12. doi: 10.1007/s12350-020-02141-0
35. Derlin T, Tóth Z, Papp L, Wisotzki C, Apostolova I, Habermann CR, et al. Correlation of inflammation assessed by 18F-FDG PET, active mineral deposition assessed by 18F-fluoride PET, and vascular calcification in atherosclerotic plaque: a dual-tracer PET/CT study. *J Nucl Med*. (2011) 52:1020–7. doi: 10.2967/jnumed.111.087452
36. Weiberg D, Thackeray JT, Daum G, Sohns JM, Kropf S, Wester HJ, et al. Clinical molecular imaging of chemokine receptor CXCR4 expression in atherosclerotic plaque using 68Ga-pentixafor PET: correlation with cardiovascular risk factors and calcified plaque burden. *J Nucl Med*. (2018) 59:266–72. doi: 10.2967/jnumed.117.196485
37. Tarkin JM, Mason JC, Fayad ZA. Imaging at the inter-face of inflammation angiogenesis by 18F-fluciclatide PET. *Heart*. (2019) 105:1845–7. doi: 10.1136/heartjnl-2019-315487
38. Dweck MR, Doris MK, Motwani M, Adamson PD, Slomka P, Dey D, et al. Imaging of coronary atherosclerosis - evolution towards new treatment strategies. *Nat Rev Cardiol*. (2016) 13:533–48. doi: 10.1038/nrcardio.2016.79
39. Choke E. Abdominal aortic aneurysm rupture is associated with increased medial neovascularization and overexpression of proangiogenic cytokines. *Arterioscler Thromb Vasc Biol*. (2006) 26:2077–82. doi: 10.1161/01.ATV.0000234944.22509.f9
40. Sadeghi MM, Krassilnikova S, Zhang J, Gharaei AA, Fassaei HR, Esmailzadeh L. Detection of injury-induced vascular remodeling by targeting activated alphavbeta3 integrin *in vivo*. *Circulation*. (2004) 110:84–90. doi: 10.1161/01.CIR.0000133319.84326.70
41. Haubner R, Kuhnast B, Mang C, Weber WA, Kessler H, Wester HJ, et al. [18F]Galacto-RGD: synthesis, radiolabeling, metabolic stability, and radiation dose estimates. *Bioconjug Chem*. (2004) 15:61–9. doi: 10.1021/bc034170n
42. Knetsch PA, Petrik M, Griessinger CM, Rangger C, Fani M, Kesenheimer C, et al. [68Ga]NODAGA-RGD for imaging $\alpha v \beta 3$ integrin expression. *Eur J Nucl Med Mol Imaging*. (2011) 38:1303–12. doi: 10.1007/s00259-011-1778-0

43. Tarkin JM, Joshi FR, Evans NR, Chowdhury MM, Figg NL, Shah AV, et al. Detection of atherosclerotic inflammation by (68)Ga-DOTATATE PET compared to [(18)F]FDG PET imaging. *J Am Coll Cardiol.* (2017) 69:1774–91. doi: 10.1016/j.jacc.2017.01.060
44. Li X, Samnick S, Lapa C, Israel I, Buck AK, Kreissl MC, et al. 68Ga-DOTATATE PET/CT for the detection of inflammation of large arteries: correlation with 18F-FDG, calcium burden and risk factors. *EJNMMI Res.* (2012) 2:52. doi: 10.1186/2191-219X-2-52
45. Zhang X, Xiong Z, Wu Y, Cai W, Tseng JR, Gambhir SS et al. Quantitative PET imaging of tumor integrin alphavbeta3 expression with 18F-FRGD2. *J Nucl Med.* (2006) 47: 113–21.
46. Derlin T, Thiele J, Weiberg D, Thackeray JT, Püschel K, Wester HJ, et al. Evaluation of 68Ga-glutamate carboxypeptidase II ligand positron emission tomography for clinical molecular imaging of atherosclerotic plaque neovascularization. *Arterioscler Thromb Vasc Biol.* (2016) 36:2213–9. doi: 10.1161/ATVBAHA.116.307701

Conflict of Interest: The authors declare that the research was conducted in the absence of any commercial or financial relationships that could be construed as a potential conflict of interest.

Publisher's Note: All claims expressed in this article are solely those of the authors and do not necessarily represent those of their affiliated organizations, or those of the publisher, the editors and the reviewers. Any product that may be evaluated in this article, or claim that may be made by its manufacturer, is not guaranteed or endorsed by the publisher.

Copyright © 2022 Dietz, Kamani, Dunet, Fournier, Rubimbura, Testart Dardel, Schaefer, Jreige, Boughdad, Nicod Lalonde, Schaefer, Mewton, Prior and Treglia. This is an open-access article distributed under the terms of the Creative Commons Attribution License (CC BY). The use, distribution or reproduction in other forums is permitted, provided the original author(s) and the copyright owner(s) are credited and that the original publication in this journal is cited, in accordance with accepted academic practice. No use, distribution or reproduction is permitted which does not comply with these terms.